COMMUNICATION

Photoinduced electron transfer in Nano-Saturn complexes of fullerene

Received 00th January 20xx,
Accepted 00th January 20xx

DOI: 10.1039/x0xx00000x

Olga A. Stasyuk,[a] Anton J. Stasyuk,[a*] Miquel Sola,[a*] and Alexander A. Voityuk[a,b*]

The photoinduced electron transfer is studied computationally in several Saturn-shaped inclusion complexes of carbo-aromatic rings and C_{60} fullerene – $C_{72}⊃C_{60}$, $C_{96}⊃C_{60}$, $C_{120}⊃C_{60}$, and $C_{168}⊃C_{60}$. Analysis of their structural and electronic properties shows that the charge separation process is efficient in $C_{120}⊃C_{60}$ and $C_{168}⊃C_{60}$ where the host molecule resembles the conjugated [24]circulene unit. In contrast, the electron transfer is not feasible in the oligophenylene-based rings $C_{72}⊃C_{60}$ and $C_{96}⊃C_{60}$ complexes.

In the past few decades, great efforts have been made to design and manufacture compounds that can efficiently mimic natural photosynthetic systems.[1] A suitable combination of donor (D) and acceptor (A) units is the main requirement in the development of photovoltaic systems in which long-lived charge-transfer (CT) states can be generated with a high quantum yield.[2] Effective communication between D and A connected by a molecular spacer may essentially be influenced by its structural and electronic features.[3] For this reason, D-A systems that are assembled via non-covalent interactions and have no spacer are of particular interest for photo-induced electron transfer (PET).

For the last decade, complexes of fullerenes with cycloparaphenylenes (CPPs) and their π-extended analogs (so-called nanorings and nanobelts) have attracted a significant attention due to their properties arising from a distorted and strained aromatic system, and radially oriented π-orbitals.[4] The CPPs complexes have relatively high binding constants so that many of them can be isolated and structurally characterized. The photophysical properties of the complexes can be varied significantly by changing both the inner and outer subunits. The electron transfer capability of certain systems makes them a promising platform for the development of photovoltaic devices.[5] A rather unusual type of the host-guest compounds in which the disc-shaped ring of the host resembles the rings of the planet Saturn. The first example of such complexes assembled by C_{60} and cyclohexabiphenylene was shown by Kigure *et al.* and was termed "nano-Saturn".[6] In contrast to other types fullerene complexes, not much is known about the nano-Saturn systems because of their relatively low stability caused by a smaller contact area between the host and guest molecules.[7]

All known nano-Saturn complexes can be divided into two groups depending on the ring nature: (1) macrocycles based on heteroaromatic molecules, e.g. oligothiophenes[8] and Cu-methylimidazolate assemblies[9] and and (2) macrocycle based on aromatic hydrocarbons, e.g. cyclohexabiphenylene (**$C_{72}H_{48}$**),[6] 1,3-phenylene-bridged hexameric naphthalene (**$C_{96}H_{60}$**),[10] and cyclic anthracene hexamer (**$C_{120}H_{72}$**) rings.[11] Recently synthesis of large-cavity coronoids with different inner and outer edge structures has been reported.[12] The newly synthesized [6]coronoid (**$C_{168}H_{60}$**) is a macrocyclic conjugated hydrocarbon which consists of circularly fused benzenoid rings and has a cavity of 1.40±0.05 nm in the center. High resolution scanning tunneling and atomic force microscopy techniques reveled its flat structure. The rigid structure of **$C_{168}H_{60}$** and the cavity diameter make this ring ideal for the formation of a nano-Saturn complex with **C_{60}** fullerene, **$C_{168}⊃C_{60}$**.

In this work, we report electronic properties of four Saturn-shaped complexes **$C_{72}⊃C_{60}$**, **$C_{96}⊃C_{60}$**, **$C_{120}⊃C_{60}$**, and **$C_{168}⊃C_{60}$** (Figure 1), and explore their ability for photoinduced electron transfer. The non-covalent interactions between the host and guest fragments are studied using the topological analysis performed using the Bader Atoms in Molecules theory (QTAIM) and the reduced density gradient non-covalent index (RDG NCI). The four structures under consideration can be divided into two groups based on the structural motif of the ring (1)

[a)] *Dr. O. A. Stasyuk, Dr. A. J. Stasyuk, Prof. Dr. M. Solà and, Prof. Dr. A. A. Voityuk*
Institute of Computational Chemistry and Catalysis and Department of Chemistry
University of Girona
C/ M. Aurèlia Capmany, 69, 17003 Girona, Spain.
E-mail: antony.stasuk@gmail.com
E-mail: miquel.sola@udg.edu
E-mail: alexander.voityuk@icrea.cat
[b)] *Prof. Dr. A. A. Voityuk*
ICREA, Pg. Lluís Companys 23, 08010 Barcelona, Spain.
Electronic Supplementary Information (ESI) available: full computational details, supporting figures and tables. See DOI: 10.1039/x0xx00000x

oligophenylene rings, which consist of alternating six *m*-phenylene and six *p*-phenylene units (**$C_{72}H_{48}$**), or its structural analog with naphthalene-1,4-diyl units (**$C_{96}H_{60}$**) and (2) [24]circulene-like rings, hexamer of anthracene-2,7-diyl units (**$C_{120}H_{72}$**) and [6]coronoid (**$C_{168}H_{60}$**). The last ring is a highly conjugated hexamer of 14-phenylbenzo[*m*]tetraphene. The formation of nano-Saturn systems were previously reported for **$C_{72}H_{48}$**, **$C_{96}H_{60}$**, and **$C_{120}H_{72}$**.[9-11] The structural similarity of these rings and the newly synthesized [6]coronoid encouraged us to compare their response to photoexcitation. We consider 1:1 complexes of the rings with **C_{60}** in their equilibrium geometries. The structures (see Figure 1) were optimized using the B3LYP-D3(BJ)/def2-SVP scheme. The excited state calculations were performed using the time-dependent DFT formalism with the range-separated CAM-B3LYP functional[13] (computational details are provided in the SI).

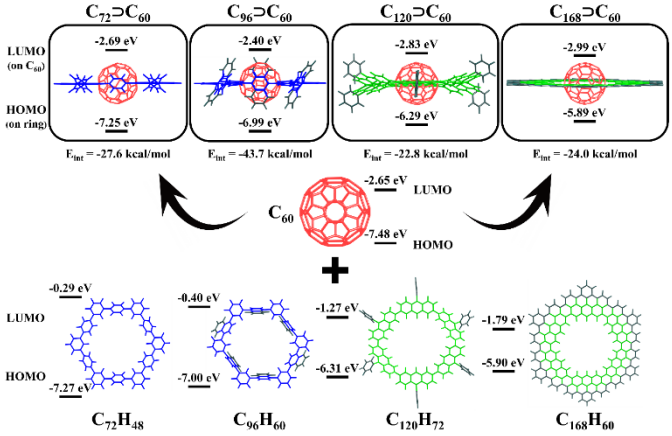

Figure 1. HOMO and LUMO energies of the host and guest molecules and their complexes.

As seen from Figure 1, the HOMO of the complexes is localized on the ring and its energy is similar to that of the host molecule. LUMO is localized on **C_{60}** in all complexes. The energy of LUMO changes by less than 0.35 eV when passing from free **C_{60}** to one of its Saturn complexes.

It is well known that even relatively small polyacenes can show a significant multi-configurational character. Biradical nature of all systems studied in this work has been tested using broken-symmetry technique. In all cases, closed-shell singlet state was found to be the ground state.

To estimate the stability of the complexes, the interaction energy (ΔE_{int}) between a ring and fullerene was computed. ΔE_{int} is found to be -27.6, -43.7, -22.8 and -24.0 kcal/mol in **C_{72}⊃C_{60}**, **C_{96}⊃C_{60}**, **C_{120}⊃C_{60}**, and **C_{168}⊃C_{60}**, respectively. Interestingly, the interaction energy in **C_{96}⊃C_{60}** is almost twice as large as that in other complexes. To understand the observed difference and gain an access to the interaction topology between the fragments, a series of QTAIM[14] calculations have been performed. Several topological parameters were calculated at the bond critical points (BCPs) (see Table S1). Two types of the host-gest interactions were revealed in **C_{72}⊃C_{60}** and **C_{96}⊃C_{60}**: the π···π interaction between the π-electron systems of the fragments and the CH···π interaction. In the case of **C_{72}⊃C_{60}**, the CH···π interactions is dominant, whereas the π···π interaction is dominant in **C_{96}⊃C_{60}** (see Table S1, SI). In view that π···π interactions are generally stronger than CH···π,[15] the binding energy in the **C_{96}⊃C_{60}** complex is larger than in **C_{72}⊃C_{60}**. In the **C_{120}⊃C_{60}** and **C_{168}⊃C_{60}** complexes, only CH···π interactions were found (see Figure S1).

Also we analyzed the non-covalent index (NCI) in the systems.[16] For the **C_{120}⊃C_{60}** and **C_{168}⊃C_{60}** complexes, the NCI isosurfaces are narrow and located strictly between CH groups of the ring and **C_{60}** unit. In case of **C_{72}⊃C_{60}**, and especially in **C_{96}⊃C_{60}** complex, the NCI isosurface is significantly wider. The reduced density gradient (RDG) plots and NCI isosurfaces are presented in Figures S2 and S3, SI. Different zones on the isosurfaces corresponds to the CH···π and π···π interactions. Their comparison enables a better understanding of the noncovalent bonding in the systems.

Simulations of the excited states were performed using the TDA-DFT method with the CAM-B3LYP-D3(BJ)/def2-SVP scheme (see SI for computational details). The guest (**C_{60}**) and the host molecule contributions to the excited state electronic density were analyzed for the lowest 100 excited states of each complex.

Table 1. Singlet excitation energies (E_x, eV), main singly excited configuration (HOMO(H)–LUMO(L)) and its weight (W), oscillator strength (f), and extent of charge separation (CT, ***e***) or exciton localization (X) in the host-guest systems.

	Supramolecular host-guest systems			
	C_{72}⊃C_{60}	**C_{96}⊃C_{60}**	**C_{120}⊃C_{60}**	**C_{168}⊃C_{60}**
	LE_1 (Fullerene C_{60})			
E_x	2.540	2.554	2.569	2.566
Transition (W)	H-3 – L (0.53)	H-2 – L+1 (0.23)	H-8 – L+1 (0.30)	H-13 – L+3 (0.29)
f	<0.001	<0.001	<0.001	<0.001
X	0.953	0.935	0.979	0.989
	LE_2 (Host)			
E_x	4.932	4.282	3.391	2.356
Transition (W)	H-1 – L+9 (0.11)	H-1 – L+7 (0.11)	H – L+6 (0.37)	H – L+8 (0.20)
f	0.011	<0.001	0.047	<0.001
X	0.940	0.964	0.992	0.995
	Most absorptive transition			
E_x	4.967	4.391	4.150	2.648
Transition (W)	H-2 – L+9 (0.10)	H-1 – L+6 (0.10)	H-5 – L+8 (0.17)	H – L+6 (0.13)
f	2.082	0.907	4.620	9.195
Localiz	**C_{72}**	**C_{96}/C_{60}**	**C_{120}**	**C_{168}**
X	0.767	0.44/0.44	0.976	0.993
	CT (Host → Fullerene C_{60})			
E_x	3.405	3.383	2.277	1.964
Transition (W)	H – L+1 (0.64)	H-3 – L+2 (0.19)	H – L (0.79)	H – L (0.96)
f	<0.001	<0.001	<0.001	<0.001
CT	0.965	0.955	0.994	0.991

Three types of excited states were identified: (1) locally excited (LE) states, where excitation is mostly localized on a single fragment with charge separation value CS < 0.1***e***. In turn, there are two types of LE excitations: LE_1 that occurs within **C_{60}**, and LE_2 that occurs within the host molecule; (2) charge transfer (CT)

states with the electron density (CS > 0.9**e**) transferred between the fragments and thus charge separation (CS) is observed and (3) mixed states with a significant contribution of both LE and CT (0.1***e*** < CS < 0.9***e***). The vertical excitation energies of **C_{72}⊃C_{60}** and **C_{96}⊃C_{60}** are found in the range from 2.5 to 5.0 eV. In both systems, LE_1 states have the lowest energy. The LE_2 states are significantly higher in energy (by 2.39 eV in **C_{72}⊃C_{60}** and 1.73 eV in **C_{96}⊃C_{60}**). Only one type of CT states, with structure $Host^+$ $Guest^-$, is found among 100 lowest states. These states lie at ~3.40 eV and are characterized by almost complete charge separation (Table 1). The CT states $Host^-$ $Guest^+$ are of higher energy (>5 eV) and were not detected within studied 100 excited states. We note that the CT transitions have weak oscillator strengths (f < 0.001) and cannot be populated by direct light absorption.

As seen from Table 1, the excited state properties of the complexes change dramatically as the size of the host molecule increases. The energy gap between LE_1 and LE_2 states becomes noticeably smaller. In particular, the LE_2 state in **C_{168}⊃C_{60}** complex becomes the lowest one, although the energy of LE_1 state remains almost unchanged. The energy of the CT state also depends strongly on the host size. The CT states in the systems correspond to electron transfer from the host ring to **C_{60}** and can be described as **$host^+$⊃C_{60}^-**. Because **$C_{120}H_{72}$** and **$C_{168}H_{60}$** are much better electron donors than **$C_{72}H_{48}$** and **$C_{96}H_{60}$** (see HOMO energies on Figure 1), the corresponding CT states have a lower energy. In fact, the CT states in **C_{120}⊃C_{60}**, and **C_{168}⊃C_{60}** become the lowest-lying excited state. Among the studied complexes, **C_{168}⊃C_{60}** seems to be the most promising. It has enormously high light absorption in the green-blue region, which makes the complex an ideal candidate for organic photovoltaics. In addition, we analyzed selected excited states with the natural transition orbital (NTO) method.[17] The NTOs representing the LE and CT states are shown in Figures S4-S7 for all studied complexes.

A well-proven COSMO-like model[18] with dichloromethane (DCM) as the solvent was applied to estimate the effect of polar environment on electronic excitations. The ground state (GS) solvation energies of **C_{72}⊃C_{60}**, **C_{96}⊃C_{60}**, **C_{120}⊃C_{60}**, and **C_{168}⊃C_{60}** are equal to -0.07, -0.09, -0.13, and -0.14 eV, respectively.

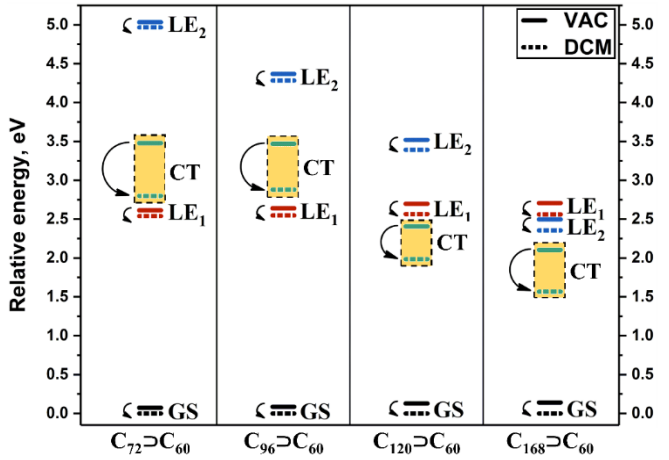

Figure 2. Relative energies (in eV) of LE and CT states for **C_{72}⊃C_{60}**, **C_{96}⊃C_{60}**, **C_{120}⊃C_{60}**, and **C_{168}⊃C_{60}** complexes computed in vacuum (VAC) and dichloromethane (DCM).

The high symmetry of the studied complexes and the ability of the host and guest molecules to effectively delocalize an extra charge suggest that solvation energies of the CT states should not be large. A change in the dipole moment by LE excitation does not exceed 1.0D. The dipole moment difference between the CT and GS states is calculated to be 22.2, 0.7, 0.8, and 11.0 D for **C_{72}⊃C_{60}**, **C_{96}⊃C_{60}**, **C_{120}⊃C_{60}**, and **C_{168}⊃C_{60}**, respectively. The solvation energies found for the CT states in the complexes are similar, -0.68, -0.59, -0.42 and -0.54 eV for **C_{72}⊃C_{60}**, **C_{96}⊃C_{60}**, **C_{120}⊃C_{60}** and **C_{168}⊃C_{60}**, respectively. The dipole moment changes and the solvation energies are listed in Table S2. Figure 2 shows the solvent effects on the LE and CT excitations in the complexes. The solvent stabilization of the CT state in **C_{72}⊃C_{60}** and **C_{96}⊃C_{60}** is insufficient to reorder the CT and LE states when passing from the gas phase to the DCM solution. However, the CT states in **C_{120}⊃C_{60}** and **C_{168}⊃C_{60}** are already the lowest and the gap between the LE_1 and CT states increases as these complexes are solvated. Thus, the population of the CT states due to electron transfer between the host and guest molecules is expected to be more efficient in the solvent (provided that the reaction remains in the normal Marcus region).

As expected, the CT states in the complexes are characterized by a very weak oscillator strength and therefore cannot be effectively populated by light absorption. However, they can be generated by the decay of the lowest LE states. The semi-classical method proposed by Ulstrup and Jortner[19] was used to compute the rate for charge separation and charge recombination. The rate is controlled by four parameters: electronic coupling $|V_{ij}|$ of the initial and the final states, solvation reorganization energy λ_s, reaction Gibbs energy ΔG^0, and effective Huang-Rhys factor S_{eff} as a function of internal reorganization energy λ_i (for details see the methodological section in SI). The rates were computed using the effective frequency of 1600 cm^{-1}, which corresponds to the stretching of C=C bonds. Note that the calculated ET rate does not change significantly by changing the effective frequency from 1400 to 1800 cm^{-1}.

Table 2. Gibbs energy ΔG^0, electronic coupling $|V_{ij}|$, solvent (λ_s) and internal (λ_i) reorganization energy, and the ET rate k_x (in s^{-1}) for CS and CR processes for **C_{72}⊃C_{60}**, **C_{96}⊃C_{60}**, **C_{120}⊃C_{60}**, and **C_{168}⊃C_{60}** in DCM.

System	Trans.	ΔG^0,[a] eV	$\lvert V_{ij}\rvert$, eV	λ_i[b]	λ_s	k_x, s^{-1}
C_{72}⊃C_{60}	$LE_1 \rightarrow CT$	0.259	$6.65\cdot10^{-3}$	0.268	0.374	$3.61\cdot10^{7}$
C_{96}⊃C_{60}	$LE_1 \rightarrow CT$	0.332	$8.10\cdot10^{-4}$	0.260	0.266	$4.45\cdot10^{4}$
C_{120}⊃C_{60}	$LE_1 \rightarrow CT$	-0.289	$1.27\cdot10^{-4}$	0.171	0.273	$5.72\cdot10^{8}$
	$CT \rightarrow GS$	-1.987	$3.49\cdot10^{-4}$	0.189	0.273	$1.60\cdot10^{4}$
C_{168}⊃C_{60}	$LE_1 \rightarrow CT$	-0.788	$7.93\cdot10^{-4}$	0.105	0.351	$2.77\cdot10^{9}$
	$CT \rightarrow GS$	-1.567	$9.47\cdot10^{-5}$	0.118	0.351	$3.57\cdot10^{4}$

[a] Gibbs energy difference between the final and initial states. [b] Internal reorganization energy defines effective Huang-Rhys factor $S_{eff} = \lambda_i/\hbar\omega_{eff}$, where $\hbar\omega_{eff}$ set to 1600 cm^{-1}

The systems are characterized by a relatively small internal reorganization energy, which ranges from 0.10 to 0.27 eV. For instance, the contribution of the host molecule into λ_i of **C_{168}⊃C_{60}** complex, is as small as 0.012 eV, which is due to a high delocalization of the positive charge within the molecule **C_{168}**. The charge separation reaction in **C_{72}⊃C_{60}** and **C_{96}⊃C_{60}** has a

positive Gibbs energy and, therefore, is slow. The estimated rate is $3.61 \cdot 10^7$ and $4.45 \cdot 10^4$ s^{-1}, respectively (see Table 2).

The photoinduced electron transfer in **C_{120}⊃C_{60}** occurs in normal Marcus regime ($|\Delta G^0| < \lambda$) on the nanosecond time scale with the characteristic time τ_{ET} of 1.74 ns. For **C_{168}⊃C_{60}**, the reaction takes place in inverted Marcus regime ($|\Delta G^0| > \lambda$) with τ_{ET} =0.360 ns. The charge recombination reaction for both **C_{120}⊃C_{60}** and **C_{168}⊃C_{60}** takes place in the deep inverted Marcus region ($|\Delta G^0| \gg \lambda$) and occurs on the microsecond time scale (the corresponding τ_{CR} is equal to 28 and 63 μs).

Summarizing, the photoinduced charge separation and charge recombination reactions have been studied in the nano-Saturn complexes **C_{72}⊃C_{60}**, **C_{96}⊃C_{60}**, **C_{120}⊃C_{60}**, and **C_{168}⊃C_{60}** using the TD-DFT approach. The inclusion complex **C_{168}⊃C_{60}** based on π-extended [6]coronoid is the first hydrocarbon-based nano-Saturn complex with truly flat ring. It is characterized by a high intensity of the light absorption in the visible spectrum and has promising PET properties. The CT state **C_{168}^{+}⊃C_{60}^{-}** can be populated on the sub-nanosecond time scale. The charge separation in the structurally similar complex **C_{120}⊃C_{60}** has been found to be slightly less efficient. The electron transfer in the oligophenylene-based complexes **C_{72}⊃C_{60}** and **C_{96}⊃C_{60}** is much slower due to its negative driving force.

We are grateful for financial support from the Spanish MINECO (Network RED2018-102815-T, project CTQ2017-85341-P, and Juan de la Cierva formación contract FJCI-2016-29448 to A.J.S. and FJCI-2017-32757 to O.A.S.) and the Catalan DIUE (2017SGR39). A.J.S. and M.S. are grateful for the computer resources at LaPalma (IAC) and the technical support provided by Canary Islands Institute of Astrophysics (RES-QSB-2020-3-0020).

Conflicts of interest

There are no conflicts to declare.

Notes and references

1 (a) G. Bottari, G. de la Torre, D. M. Guldi and T. Torres, *Chem. Rev.*, 2010, **110**, 6768-6816. (b) R. L. House, N. Y. M. Iha, R. L. Coppo, L. Alibabaei, B. D. Sherman, P. Kang, M. K. Brennaman, P. G. Hoertz and T. J. Meyer, *J. Photochem. Photobiol., C*, 2015, **25**, 32-45.

2 (a) Y. Lin, Y. Li and X. Zhan, *Chem. Soc. Rev.*, 2012, **41**, 4245-4272. (b) H. Bronstein, C. B. Nielsen, B. C. Schroeder and I. McCulloch, *Nat. Rev. Chem.*, 2020, **4**, 66-77.

3 (a) D. T. Gryko, C. Clausen, K. M. Roth, N. Dontha, D. F. Bocian, W. G. Kuhr and J. S. Lindsey, *J. Org. Chem.*, 2000, **65**, 7345-7355. (b) L. E. Greene, R. Lincoln and G. Cosa, *Photochem. Photobiol.*, 2019, **95**, 192-201.

4 (a) T. Iwamoto, Y. Watanabe, Y. Sakamoto, T. Suzuki and S. Yamago, *J. Am. Chem. Soc.*, 2011, **133**, 8354-8361. (b) D. Lu, Q. Huang, S. Wang, J. Wang, P. Huang and P. Du, *Front. Chem.*, 2019, **7**, 668. (c) D. Wu, W. Cheng, X. Ban and J. Xia, *Asian J. Org. Chem.*, 2018, **7**, 2161-2181.

5 (a) H. Ueno, T. Nishihara, Y. Segawa and K. Itami, *Angew. Chem. Int. Ed.*, 2015, **54**, 3707-3711. (b) Y. Xu, B. Wang, R. Kaur, M. B. Minameyer, M. Bothe, T. Drewello, D. M. Guldi and M. von Delius, *Angew. Chem. Int. Ed.*, 2018, **57**, 11549-11553. (c) Q. Huang, G. Zhuang, H. Jia, M. Qian, S. Cui, S. Yang and P. Du, *Angew. Chem. Int. Ed.*, 2019, **58**, 6244-6249. (d) A. J. Stasyuk, O. A. Stasyuk, M. Solà and A. A. Voityuk, *Chem. Commun.*, 2019, **55**, 11195-11198.

6 S. Kigure, H. Omachi, H. Shinohara and S. Okada, *J. Phys. Chem. C*, 2015, **119**, 8931-8936.

7 (a) S. Toyota and E. Tsurumaki, *Chem.- Eur. J.*, 2019, **25**, 6878-6890. (b) H. U. Rehman, N. A. McKee and M. L. McKee, *J. Comp. Chem.*, 2016, **37**, 194-209.

8 (a) H. Shimizu, J. D. Cojal González, M. Hasegawa, T. Nishinaga, T. Haque, M. Takase, H. Otani, J. P. Rabe and M. Iyoda, *J. Am. Chem. Soc.*, 2015, **137**, 3877-3885. (b) H. Shimizu, K. H. Park, H. Otani, S. Aoyagi, T. Nishinaga, Y. Aso, D. Kim and M. Iyoda, *Chem. -Eur. J.*, 2018, **24**, 3793-3801. (c) M. Iyoda, H. Shimizu, S. Aoyagi, H. Okada, B. Zhou and Y. Matsuo, *Can. J. Chem.*, 2016, **95**, 315-319.

9 S.-Z. Zhan, J.-H. Li, G.-H. Zhang, M.-D. Li, S. Sun, J. Zheng, G.-H. Ning, M. Li, D.-B. Kuang, X.-D. Wang and D. Li, *Chem. Commun.*, 2020, **56**, 3325-3328.

10 P. Mei, A. Matsumoto, H. Hayashi, M. Suzuki, N. Aratani and H. Yamada, *RSC Adv.*, 2018, **8**, 20872-20876.

11 (a) Y. Yamamoto, E. Tsurumaki, K. Wakamatsu and S. Toyota, *Angew. Chem. Int. Ed.*, 2018, **57**, 8199-8202. (b) S. Toyota, Y. Yamamoto, K. Wakamatsu, E. Tsurumaki and A. Muñoz-Castro, *Bull. Chem. Soc. Jpn.*, 2019, **92**, 1721-1728.

12 M. Di Giovannantonio, X. Yao, K. Eimre, J. I. Urgel, P. Ruffieux, C. A. Pignedoli, K. Müllen, R. Fasel and A. Narita, *J. Am. Chem. Soc.*, 2020, **142**, 12046-12050.

13 T. Yanai, D. P. Tew and N. C. Handy, *Chem. Phys. Lett.* 2004, **393**, 51-57.

14 R. F. W. Bader, *Chem. Rev.*, 1991, **91**, 893-928.

15 (a) J. Wang and L.Yao, *Sci. Rep.*, 2019, **9**, 20149. (b) R. Thakuria, N. K. Nath and B. K. Saha, *Cryst. Growth Des.* 2019, **19**, 523–528.

16 E. R. Johnson, S. Keinan, P. Mori-Sánchez, J. Contreras-García, A. J. Cohen and W. Yang, *J. Am. Chem. Soc.*, 2010, **132**, 6498-6506.

17 M. Head-Gordon, A. M. Grana, D. Maurice and C. A. White, *J. Phys. Chem.*, 1995, **99**, 14261-14270.

18 (a) B. Mennucci, *WIREs Comput. Mol. Sci.*, 2012, **2**, 386-404. (b) A. J. Stasyuk, O. A. Stasyuk, S. Filippone, N. Martin, M. Solà and A. A. Voityuk, *Chem. Eur. J.*, 2018, **24**, 13020-13025. (c) O. A. Stasyuk, A. J. Stasyuk, A. A. Voityuk and M. Solà, *J. Org. Chem.* 2020, **85**, 11721–11731.

19 (a) J. Ulstrup and J. Jortner, *J. Chem. Phys.*, 1975, **63**, 4358-4368.

